ORIGINAL RESEARCH ARTICLE

Determination of gold nanoparticles sizes from their plasmon resonance within the optical spectrum.

Gitonga Mbae John[1], Simon Waweru Mugo[1], James Mbiyu Ngaruiya[1],

[1]Department of Physics, Jomo Kenyatta University of Agriculture and Technology (JKUAT), Nairobi Kenya

Corresponding author email: ***mbaejoni@gmail.com***

Abstract

Nanoparticles have exciting properties that can be tailored by altering their size, density, and shape. A number of important properties of the nanoparticles have been investigated for various applications. One such property that is strongly affected by nanoparticle size is localised surface plasmon resonance (LSPR). The resonance from metal nanoparticles has been used in dye-sensitised solar cells to improve their performance. In this work, the dependence of plasmonic properties on nanoparticle sizes is shown. The gold nanoparticles were prepared using a reduction process where hydrogen tetrachloroaurate acid was used as the base gold salt and reduced by sodium citrate at different molarities ranging from 0.015 to 0.035 mol/L. The method produces monodispersed nanoparticles whose sizes are sensitive to the concentration of chemicals used and the completeness of the reduction process. The process took approximately 18 minutes, and the colour changed from pale yellow to wine-red. The absorbance of the resulting gold nanoparticles was determined using a UV-Vis spectrophotometer within the range of 300 nm to 800 nm. The LSPR peaks were found to occur within 518 nm to 520 nm, and from a Gaussian fit, the FWHM ranged from 45.5 to 51.0 nm. The absorption peaks had a narrow range of 14 nm over the range of molarity of sodium citrate. A high molarity concentration of 0.035 mol/L produced a small particle with a diameter of 17.04 nm, while a low concentration of 0.015 mol/L produced a size of 26.55 nm. The interaction of electrons in the specific orbitals, sp- and d-, of nanoparticles exhibited pronounced multiple resonances with the reduction of nanoparticle sizes.

Keywords: Localized surface plasmon resonance (LSPR), Full width at half maximum (FWHM), Gold nanoparticles (AuNP), Sodium citrate

1.0 Introduction

The rising motivation in research on nanoparticles is due to their famous quantum size, which makes them exhibit unique properties such as LSPR from their bulk counterparts (Florian *et al*., 2013; Jeevanandam *et al*., 2018). These properties can be tailored by controlling the nanoparticle size, shape, and concertation during their synthesis (Jeevanandam *et al*., 2018). One of the major properties of nanoparticles is their strong absorption of the optical spectrum (Jeevanandam *et al*., 2018; Lance *et al*., 2003). This has led to the wide spread application of nanoparticles in the development of nano-devices for various applications such as physical, biomedical, and biological (Wasike *et al*., 2014: Florian *et al*., 2013; Mandal *et al*., 2011).

ISSN 1561-7645 (online)
doi: 10.4314/jagst.v22i4.6

A number of metal NP synthesis protocols have been developed. An approach to achieve a monodispersed metal NP is vital to achieving a catalytic action with high accuracy (Liu & Corma, 2018). In the classical nucleation theory approach, a chemical reduction process with a reducing agent of low crystallisation potential is commonly used. In order to synthesise gold nanoparticles using a similar approach, Au(III) was introduced in deionized water in the form of hydrogen tetrachloroaurate (Turkevich *et al*., 1951). The synthesis of AuNP with different sizes during a reduction process could be achieved in a number of ways. A reducing agent plays a critical role during chemical routines as it also serves as a capping agent and a pH mediator (Mulati *et al*., 2012; Ajitha *et al*., 2016). The variation in concentration levels of a given reducing agent, which was calculated in accordance with equation 1, gives rise to AuNPs of different sizes (Turkevich *et al*., 1951; Ajitha *et al*., 2016).

$$C = \frac{m}{v} \times \frac{1}{MW} \ldots \ldots \ldots \ldots \ldots \ldots (1)$$

Where m is the mass of the solute, v is the volume of the solution in litres, and mw is the molar weight.

The UV-Vis technique offers a reliable method of obtaining absorbance data from NPs useful in the evaluation of LSPR peak wavelength. Photons incident on a material can be transmitted, scattered, or absorbed. The extent of photon absorption depends on the bandgap of the material, and the absorbance scatter reveals whether there are LSPR peaks within the material (Wormell & Rodger, 2013). The LSPR peak range determines whether the NPs were monodispersed or polydispersed. As the sizes of NPs decrease during the nucleation process, the LSPR undergoes a blue shift (Piella *et al*., 2016; Zorić et al., 2011). There exists a strong relationship between LSPR peaks and FWHM values, which reveal the lifetime of SPR from a nanoparticle (Ringe *et al*., 2012). The variation of LSPR wavelength and FWHM in a monodispersed system can be used to determine the NP sizes, as shown in equation 2 (11).

$$\lambda_{LSPR} = \lambda_0 + L_1 \exp(L_2 D) \ldots \ldots (2)$$

Where L_1 and L_2 are fit parameters and D the nanoparticle size.

This variation has been used further to explain the NP size dependence on the pH of the reducing agent in a reduction process (Iravani *et al*., 2014). The LSPR peaks were obtained from absorbance spectra within the optical region of the spectrum. FWHM values for each peak were obtained by fitting a Gaussian curve to each peak. These plasmonic properties were used in calculating the AuNP sizes for different molarities of reducing agents.

2.0 Materials and methods

The glassware used was cleaned by first soaking it in a boiling solution of weak sodium carbonate for 10 minutes to remove any grease or fat. Then they were rinsed with acetone, followed by deionized water. They were dried by placing them in the oven, heated to 110°C for 6 hours. Hydrogen tetrachroloaurate (III) trihydrate ($HAuCl_4.3H_2O$, 99.9%), sodium citrate

ISSN 1561-7645 (online)
doi: 10.4314/jagst.v22i4.6

($Na_3C_6H_5O_7$, 99.0%), citric acid, and hydrochloric acid were sourced from Sigma-Aldrich and were of analytical grade.

AuNPs used in this study were synthesised using the Turkervich method (Turkevich *et al*., 1951). Gold salt, 0.1 wt% hydrogen tetrachloroaurate, was used as the base of AuNPs. It was dissolved in deionized water, and the solution topped out at 50 ml. The solution was heated to a boil under vigorous magnetic stirring. A reduction bumper, Na_3Ctr was introduced to the solution, and heating continued for 23 minutes until no further colour change was noted. The solution was cooled to room temperature under magnetic stirring. The process was repeated for different pH values of Na_3Ctr.

The absorbance data of the colloidal AuNPs was determined using a UV-Vis spectrophotometer, and OriginPro8 software was used to plot the absorbance spectra. A Gaussian curve was fitted to each of the absorption peaks to obtain the corresponding plasmon wavelength used in the determination of AuNP sizes as in equation 2.

3.0 Results and discussion

Figure 1 shows a linear fit for the molarity of reducing buffer and their corresponding pH values. The rate of change was uniform at 100L/mMol. Citrate

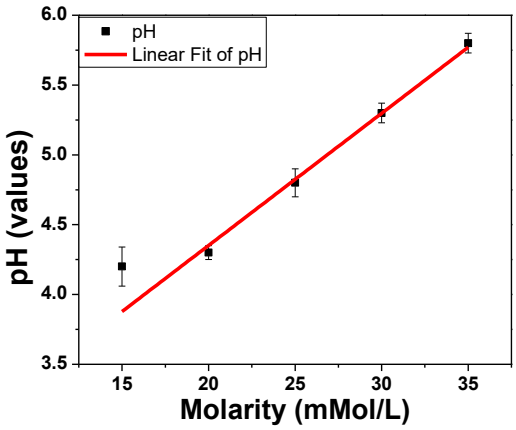

Figure 1: Plot of pH versus molarity of sodium

Thus, the reducing agent had a high reduction potential with low crystallisation within the considered concentrations, and no solubility limits were reached. This not only made it an effective reducing agent but also a good capping agent during the chemical process (Ibrahim et al., 2019). The spike in pH value at low molarity is due to precipitation of Na_3Ctr. The variation of pH in a reducing agent during a chemical process plays a key role in controlling the morphology and sizes of NPs (Ibrahim et al., 2019; Patungwasa et al., 2008).

During the process of reduction, the AuNP nucleation phases were presented by colour changes within a period of 18 minutes. The addition of Na_3Ctr to the $HAuCl_4.3H_2O$ while heating under vigorous magnetic stirring shows the reduction of Au(III) into colourless Au(0). The dark violet colour attained within 13 minutes was due to the formation of Au nanowires as an intermediate

ISSN 1561-7645 (online)
doi: 10.4314/jagst.v22i4.6

step during the nucleation process. This is consistent with Au nanowires absorbing most of the optical spectrum, giving the solution a dark violet colour (Pong et al., 2007).

Continued heating made the solution supersaturated, which led to the formation of spherical AuNPs. A blue shift in wavelength occurs with the AuNPs absorbing light in the blue-green regions, giving the solution a wine-red colour.

Absorbance data from UV-Vis confirmed the presence of AuNPs. Figure 3 shows absorbance spectra for colloidal AuNPs synthesised at different molarities of $Na_3C_6H_5O_7$. The LSPR peaks ranged from 518.2 nm to 521.0 nm as the molarity of the reducing agent was increased from 15 mM to 35 mM.The peaks exhibited a narrow shift of approximately 7.3 nm, a clear indication that NPs were monodispersed (Peng et al., 2010). The presence of NPs was further tested using a laser beam, and Tyndall scattering was observed with all the samples obtained from varied molarities of reducing agents. For NPs with diameters below 30 nm, the position of the LSPR peak is affected by interband transitions and electron density on the surface of the NP (Shuichi et al., 2012; Wilcoxon et al., 2001).

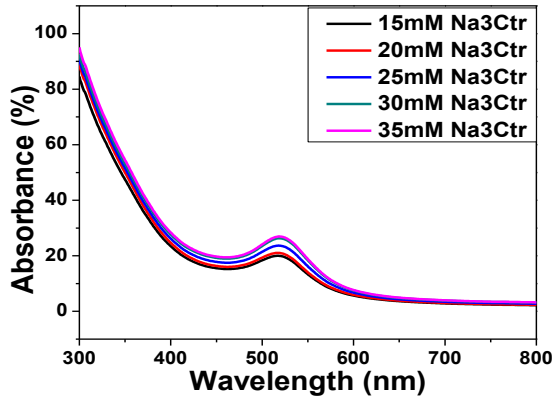

Figure 3: Absorbance versus wavelength at selected molarities of Na_3Ctr

For AuNPs, the interband transitions between the sp- and d-bands with a sustained resonance of approximately 2.37 eV, which corresponds to a wavelength range of 520 nm, were noted. In order to determine the FWHM values, a Gaussian curve was fitted to each absorption peak.

Figure 4 shows a Gaussian fit on 35 mM Na_3Ctr spectra, which gave a FWHM value of 45.5 nm. The process was repeated for other molarities, and the values of FWHM obtained are recorded in Table 1. The values ranged from 45.51 nm to 51.04 nm, which were very low compared to the wavelength of the incident photons. Low FWHM values give high integrity features to the AuNPs, hence a better signal-to-noise ratio.

ISSN 1561-7645 (online)
doi: 10.4314/jagst.v22i4.6

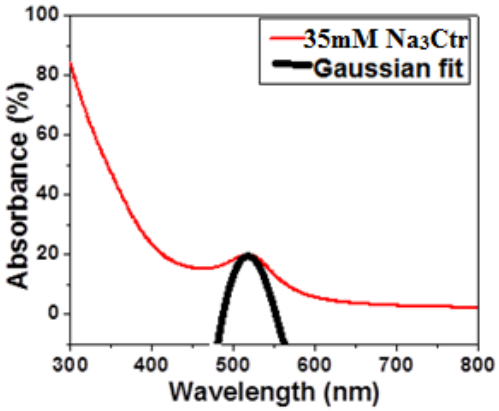

Figure 4: Gaussian fit on a curve plot of absorbance versus wavelength on selected spectra

The life of any SPR depends on the width of the absorption peak. The smallest width corresponded to a peak at 35 mM Na_3Ctr which represents NPs having the smallest size. The FWHM and the LSPR peaks depend on aggregation within the NPs, with the FWHM used to determine the dispersity of NPs.

Table 1: Variation of LSPR peak with FWHM

Molarity (mMol/L)	LSPR peak (nm)	FWHM (nm)
15	521.0	51.04
20	520.0	48.01
25	519.0	45.60
30	518.5	45.54
35	518.2	45.51

AuNP sizes were determined from their absorbance data within the optical spectrum. The sizes were found to decrease with an increase in the molarity of the reducing agent, as shown in figure 5. The Boltzmann fit within the range of nanoparticle sizes had a coefficient of 0.20788. The rate of change of nanoparticle sizes at low and high molarities was small, whereby the sizes decreased from 26 nm to 17 nm, as obtained from equation 2, while the molarity increased from 15 mM to 35 mM. The sizes of AuNP obtained due to different molarities were below 30 nm, which was consistent with AuNP obtained from the variation of volume of the reduction agent (Ngumbi et al., 2019). The decrease in size is attributed to a complete reduction process, the LSPR dipole coupling effect, and electron interchange at NP orbits.

ISSN 1561-7645 (online)
doi: 10.4314/jagst.v22i4.6

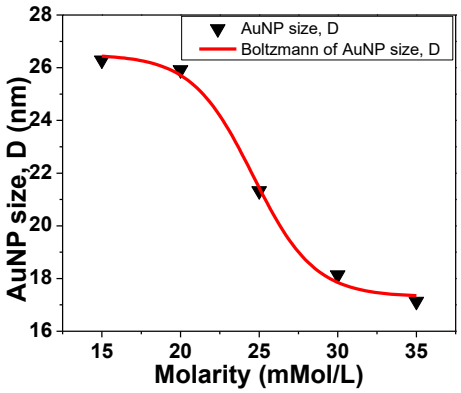

Figure 5: Variation of AuNP sizes with the molarity of reducing agent.

4.0 Conclusion

The pH values of sodium citrate used as a reducing agent were found to increase linearly with molarity. No solubility limits were attained. During the reduction process, a colour change consistent with gold nanoparticle absorption during nucleation was witnessed. Absorption peaks for AuNPs occurred at approximately 520 nm, with a narrow shift in LSPR wavelength for various concentrations being observed. The values of FWHM for all samples were relatively small, ranging from 45.51 nm to 51.04 nm, a clear indicator for quality AuNPs to foster a sustained Plasmon lifetime, making them suitable for application in photonics.

5.0 Acknowledgement

5.1 General acknowledgement

None

5.2 Funding

None

5.3 Conflict of interest

None.

5.4 Ethical consideration

None

6.0 References

Ajitha, B., Reddy, Y., Reddy, P., Hwan-Jin and Ahn, Chi Won. (2016). Role of capping agents in controlling silver nanoparticles size, antibacterial activity and potential application as optical hydrogen peroxide sensor. *RSC Advances*. 6. 36171-36179. http://dx.doi.org/10.1039/C6RA03766F

Florian J. Heiligtag, Markus Niederberger, (2013). The fascinating world of nanoparticle research. *Materials Today*, 16:7–8, 262-271. https://doi.org/10.1016/j.mattod.2013.07.004

Ibrahim K., Khalid S., and Idrees K., (2019). Nanoparticles: Properties, applications and toxicities. *Arabian Journal of Chemistry*, 12: 908-931. https://doi.org/10.1016/j.arabjc.2017.05.011

Iravani, S., Korbekandi, H., Mirmohammadi, S. V., and Zolfaghari, B. (2014). Synthesis of silver nanoparticles: chemical, physical and biological methods. *Research in pharmaceutical sciences,* 9(6), 385–406.

Jeevanandam, J., Barhoum, A., Chan, Y. S., Dufresne, A., & Danquah, M. K. (2018). Review on nanoparticles and nanostructured materials: history, sources, toxicity and regulations. *Beilstein journal of nanotechnology*, *9*, 1050–1074. https://doi.org/10.3762%2Fbjnano.9.98

Lance Kelly, Eduardo Coronado, Lin Lin Zhao, and George C. Schatz, (2003). The Optical Properties of Metal Nanoparticles: Influence of Size, Shape, and Dielectric Environment. The Journal of Physical Chemistry B 107 (3), 668-677. https://pubs.acs.org/doi/10.1021/jp026731y

Liu, L., and Corma, A. (2018). Metal Catalysts for Heterogeneous Catalysis: From Single Atoms to Nanoclusters and Nanoparticles. *Chemical reviews*, *118*(10), 4981–5079. https://pubs.acs.org/doi/10.1021/acs.chemrev.7b00776

Mandal, Gopa and Ganguly, Tapan. (2011). Applications of nanomaterials in the different fields of photosciences. *Indian Journal of Physics*. 85. 1229-1245. http://dx.doi.org/10.1007/s12648-011-0149-9

Mulati D. M. Timonah N. S. and Bjorn W. (2012). The absorption spectra of natural dyes and their suitability as a sensitiser in organic solar cell application. Journal of Agriculture, Science, and Technology, 14(1): pp. 45-61.

Ngumbi, P., Mugo, S., Ngaruiya, J., and King'ondu, C. (2019). Multiple plasmon resonances in small-sized citrate reduced gold nanoparticles. *Materials Chemistry and Physics*. 233, Pages 263-266. https://doi.org/10.1016/j.matchemphys.2019.05.077

Patungwasa, Wissanu and Hodak, Jose. (2008). pH Tunable Morphology of the Gold Nanoparticles Produced by Citrate Reduction. *Materials Chemistry and Physics*. 108. 45-54. https://doi.org/10.1016/j.matchemphys.2007.09.001

Peng, S., McMahon, J. M., Schatz, G. C., Gray, S. K., & Sun, Y. (2010). Reversing the size-dependence of surface plasmon resonances. Proceedings of the National Academy of Sciences of the United States of America, 107(33), 14530–14534. https://doi.org/10.1073/pnas.1007524107

Piella, Jordi & Bastús, Neus & Puntes, Victor. (2016). Modeling the Optical Responses of Noble Metal Nanoparticles Subjected to Physicochemical Transformations in Physiological Environments: Aggregation, Dissolution and Oxidation. *Journal of physical chemistry*, 231. 0863- 0874. http://dx.doi.org/10.1515/zpch-2016-0874

Pong, Boon-Kin & Elim, Hendry Izaac & Chong, Jian-Xiong & Ji, Wei & Trout, Bernhardt & Lee, Jim. (2007). New Insights on the Nanoparticle Growth Mechanism in the Citrate Reduction of Gold(III) Salt: Formation of the Au Nanowire Intermediate and Its Nonlinear Optical Properties. *Journal of Physical Chemistry* C 111-128. https://doi.org/10.1021/jp068666o

Ringe, Emilie & Langille, Mark & Sohn, Kwonnam & Zhang, Jian & Huang, Jiaxing & Mirkin, Chad & Duyne, Richard & Marks, Laurence. (2012). Plasmon Length: A Universal Parameter to Describe Size Effects in Gold Nanoparticles. *The Journal of Physical Chemistry Letters.* 3. 1479-1483. https://doi.org/10.1021/jz300426p

ISSN 1561-7645 (online)
doi: 10.4314/jagst.v22i4.6

Shuichi H., Daniel W., Takayuki U., (2012). Studies on the interaction of pulsed lasers with plasmonic gold nanoparticles toward light manipulation, heat management, and nanofabrication. *Journal of Photochemistry and Photobiology*, 13: 1, 28-54. https://doi.org/10.1016/j.jphotochemrev.2012.01.001

Turkevich, J., Stevenson, P. C., and Hillier, J. (1951). A study of the nucleation and growth processes in the synthesis of colloidal gold. *Discussions of the Faraday Society*, *11*, 55–75. https://doi.org/10.1039/DF9511100055

Wasike N. W. soitah T. N. Waweru S. M. and Kariuki F. N. (2014). Assessment of the solar radiation potential of the thika and Nairobi area. Journal of Agriculture, Science, and Technology, 16(1): pp. 93-105.

Wilcoxon P., Martin E., and Provencio P. (2001). Optical properties of gold and silver nanoclusters investigated by liquid chromatography. *J Chem Phys.*;115: 998–1008. http://dx.doi.org/10.1063/1.1380374

Wormell P. and Rodger A. (2013) Absorbance Spectroscopy: Overview In: Roberts G.C.K. (eds) Encyclopedia of Biophysics. *Springer*, Berlin, Heidelberg.

Zorić, I., Michael, K., Bengt and Langhammer, C. (2011). Gold, Platinum, and Aluminum Nanodisk Plasmons: Material Independence, Subradiance, and Damping Mechanisms. *ACS nano*. 5. 2535-2546. http://dx.doi.org/10.1021/nn102166t

ISSN 1561-7645 (online)
doi: 10.4314/jagst.v22i4.6